Robotica (2003) volume 21, pp. 541–554. © 2003 Cambridge University Press
DOI: 10.1017/S0263574703005046 Printed in the United Kingdom

# Kinematic and dynamic analysis of Stewart platform-based machine tool structures

K. Harib* and K. Srinivasan†

(Received in Final Form: December 31, 2002)

## SUMMARY

In this paper, an analytical study of the kinematics and dynamics of Stewart platform-based machine tool structures is presented. The kinematic study includes the derivation of closed form expressions for the inverse Jacobian matrix of the mechanism and its time derivative. An evaluation of a numerical iterative scheme for an on-line solution of the forward kinematic problem is also presented. Effects of different configurations of the unpowered joints on the angular velocities and accelerations of the links are considered. The Newton-Euler formulation is used to derive the rigid body dynamic equations. Inclusion of models for actuator dynamics and joint friction is discussed.

KEYWORDS: Stewart platform; Machine tools; Kinematics and dynamics.

## 1. INTRODUCTION

In recent years, the Stewart Platform mechanism has attracted considerable attention in view of its application to 6 degree-of-freedom machine tool structures. Such an application has been motivated by the excellent mechanical characteristics of the mechanism in terms of its higher rigidity and strength-to-weight ratio when compared to serial link manipulators, and its greater maneuverability when compared to conventional machine tool structures.

The Stewart Platform, also known as the "Gough-Stewart" Platform, was first introduced by Gough in 1956 as a tire testing machine,[1] and then by Stewart in 1965 as an aircraft simulation mechanism.[2] Since then, it has attracted considerable research interest in the context of manufacturing and robotic applications. Hunt suggested using the platform as an in-parallel robot arm.[3] Geng and Haynes experimentally explored the Stewart Platform as a vibration isolation device.[4] Recently, a number of commercial machine tools have been introduced based on the Stewart platform mechanism. Examples include the Ingersoll Hexapod, the Hexel and the Variax machining centers. As depicted in Figure 1, the Stewart Platform comprises a payload platform to which six linear actuators or struts are attached. The other ends of the struts are attached to the base. Each of the struts is attached to the platform and to the base by either a three degrees-of-freedom joint and a two degree-of-freedom joint, or by two three degrees-of-freedom joints. The linear extension and retraction of the six actuators gives the platform six degrees-of-freedom positioning capabilities, consisting of three translational and three rotational degree-of-freedom. The linear actuation could be provided either hydraulically or electrically, and usually includes a ballscrew-nut mechanism to convert motor shaft rotation to strut extension or retraction.

Fully parallel link mechanisms, which include the Stewart Platform, show kinematic characteristics different from those of serial link mechanisms. The inverse kinematic problem for Stewart Platforms, that is, determination of the joint space position or the six link lengths given the position/orientation of the platform or the Cartesian space position, is straightforward to perform. The forward kinematic problem, viz. the determination of the Cartesian space position for a given joint space position, is more demanding computationally. Both closed form solutions and numerical iterative schemes are employed, simpler closed form solutions being possible for special arrangements.[5] The forward rate kinematic and forward acceleration kinematic problems, on the other hand, are linear, requiring solution of linear system of equations involving the inverse Jacobian matrix and its time derivative. Closed form expressions for these matrices are necessary for transforming dynamic

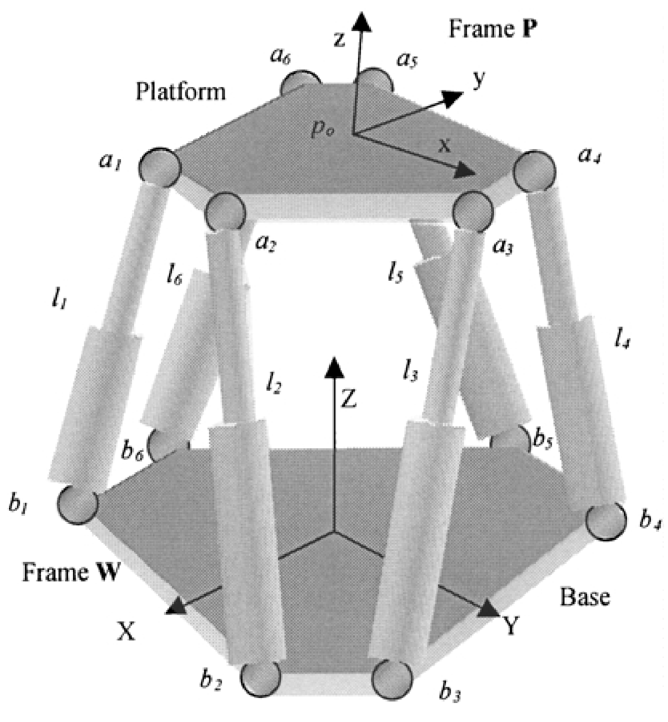


Fig. 1. Stewart platform mechanism.

* Department of Mechanical Engineering, United Arab Emirates University, Al-Ain (United Arab Emirates)
† Department of Mechanical Engineering, The Ohio State University, Columbus, Ohio 43210 (USA)

equations between joint space and Cartesian space coordinates.

Unlike serial link manipulators, dynamic models for Stewart Platforms as a class of fully parallel link mechanisms have not been fully developed. In the reported literature on the dynamic modeling of Stewart Platforms, both the Newton-Euler formulation[6–8] and the Lagrangian formulation[9–11] have been used. These works primarily consider the rigid body dynamics of Stewart Platform mechanisms. Most of these works used simplifying assumptions, and none have considered the effects of the types of strut end joints on the kinematic and dynamic analysis of the struts. Ji,[7] and Dasgupta and Mruthyunjaya,[8] did take note of such effects in their dynamic analysis using the Newton-Euler formulation. However, their assumption that there is no axial rotation of the strut when a universal joint is used for the base joint is only an approximation.

In this paper, we present a kinematic and dynamic analysis of a Stewart Platform machine tool structure using the Newton-Euler formulation. The machine tool structure is closely related to the Octahedral Hexapod manufactured by Ingersoll. The kinematic study includes determination of closed form expressions for the inverse Jacobian matrix and its time derivatives. The effects of having different configurations of strut end joints on the kinematics and dynamics of the mechanism are more accurately modeled. The inclusion of actuator dynamics and joint friction in the derived rigid body dynamic equations is also discussed.

## 2. COORDINATE SYSTEM ASSIGNMENT

The moving platform of the Stewart Platform mechanism is a rigid body that possesses six degrees of freedom. Therefore, to fully describe its position and orientation, six coordinates are needed. Three of these coordinates are positional displacements that locate the position of a reference point in the moving platform with reference to a fixed coordinate system. The other three coordinates are angular displacements that describe the orientation of the moving platform with reference to a nonrotating coordinate system. Euler angles are widely used to represent rigid body kinematics and dynamics. In this work, we use a set of Euler angles ($\phi$, $\theta$, $\psi$) which uniquely determine the orientation of a rigid body after the following sequence of rotations (see Figure 2):

- a rotation $\phi$ about the Z′-axis of the moving coordinate system.
- rotation $\theta$ about the x′-axis of the moving coordinate system.
- a rotation $\psi$ about the z″-axis of the moving coordinate system.

The frame X′Y′Z′ in Figure 2 is a nonrotating coordinate system that translates with the rigid body while frame xyz is a body coordinate system that both rotates and translates with the rigid body. Frames x′y′z′ and x″y″z″ are intermediate coordinate systems which are useful in performing the analysis in the next section. From the figure, we see that $\theta$ is always the angle between the z and Z′ axes. Also, with this representation, a rotation with angle $\psi$ will be a redundant degree of freedom in 5-axis machining applications, if axis z of the platform frame is chosen to coincide with the axis of the spindle of the machine tool.

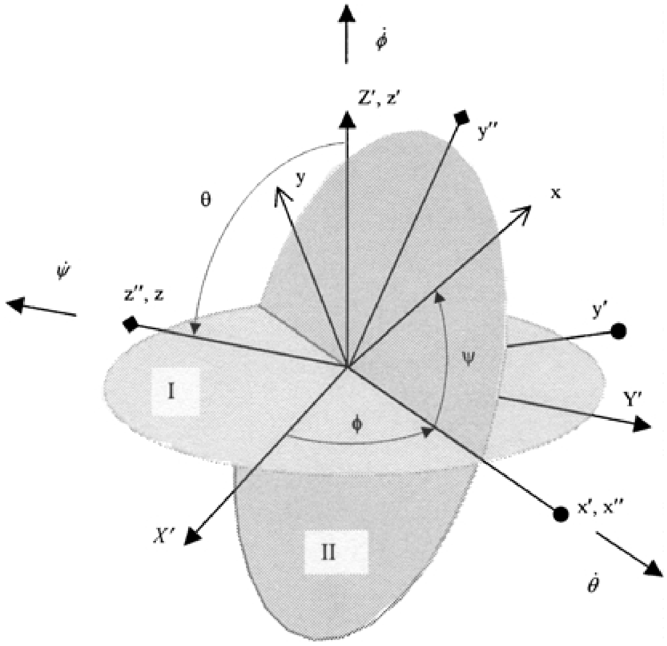


Fig. 2. Euler angles z-x-z.

Since each of the six links of the Stewart Platform is attached to the base and the moving platform at known points, the joint space kinematics of the mechanism are easily determined if the moving platform position and orientation are known. This explains the simplicity of the inverse kinematic problem for this type of mechanism. To describe the kinematics of the moving platform, we will need two coordinate systems as depicted in Figure 1. The world coordinate frame **W** is fixed to the base while the coordinate frame **P** is attached to the moving platform at a reference point $p_o$. The position of frame **P** is specified with reference to frame **W** by a vector $x=(X, Y, Z)^T$ which gives the coordinates of point $p_o$ with reference to frame **W**. The orientation of frame **P** is described with reference to frame **W** by a rotation matrix ${}^W\boldsymbol{R}_P=(\boldsymbol{r}_1, \boldsymbol{r}_2, \boldsymbol{r}_3)$, where $\boldsymbol{r}_1$, $\boldsymbol{r}_2$ and $\boldsymbol{r}_3$ are, respectively, $3\times 1$ unit vectors along the axes of frame **P** and described with reference to frame **W**. The rotation matrix ${}^W\boldsymbol{R}_P$ is derived in term of the three Euler angles in the next section.

We define a generalized coordinate vector $\boldsymbol{q}$, whose elements are the six variables chosen to describe the position and orientation of the platform, as

$$\boldsymbol{q}=(X, Y, Z, \phi, \theta, \psi)^T \tag{1}$$

The joint space coordinate vector $\boldsymbol{l}$ is defined as

$$\boldsymbol{l}=(l_1, l_2, l_3, l_4, l_5, l_6)^T \tag{2}$$

where $l_i$ for $i=1, \ldots, 6$ are the lengths of the six numbered links of the Stewart Platform. In the following sections, the mapping between these two sets of coordinates and their time derivatives will be presented.

## 3. KINEMATICS OF THE MOVING PLAFFORM

The mapping between the x-y-z coordinates (or the platform coordinate frame **P**) and the X′-Y′-Z′ coordinates is

https://doi.org/10.1017/S0263574703005046 Published online by Cambridge University Press

achieved through a $3\times3$ rotation matrix ${}^{W}\boldsymbol{R}_P$ involving the three Euler angles $\phi$, $\theta$, $\psi$. ${}^{W}\boldsymbol{R}_P$ is given for the used Euler angle representation as

$$^{W}\boldsymbol{R}_P=\begin{pmatrix} c\psi c\phi-c\theta s\phi s\psi & -s\psi c\phi-c\theta s\phi c\psi & s\theta s\phi \\ c\psi s\phi+c\theta c\phi s\psi & -s\psi s\phi+c\theta c\phi c\psi & -s\theta c\phi \\ s\psi s\theta & c\psi s\theta & c\theta \end{pmatrix} \tag{3}$$

where $c$ and $s$ denote cosine and sine respectively.

Before proceeding to the inverse kinematic problem, it is useful to express the angular velocity $\omega=(\omega_X, \omega_Y, \omega_Z)^T$ and angular acceleration $\alpha=(\alpha_X, \alpha_Y, \alpha_Z)^T$ of the moving platform with reference to frame **W** as functions of the first and second time derivatives of the Euler angles ($\dot\phi$, $\dot\theta$, $\dot\psi$) and ($\ddot\phi$, $\ddot\theta$, $\ddot\psi$). Referring back to Figure 2, the moving platform has an angular velocity component $\dot\phi$ along the Z′ axis, an angular velocity component $\dot\theta$ along the x′ axis, and an angular velocity component $\dot\psi$ along the z″ axis. Resolving these components along the axes of frame **W** we obtain

$$\omega=\begin{pmatrix}\omega_X\\ \omega_y\\ \omega_Z\end{pmatrix}=\begin{pmatrix}0 & c\phi & s\phi c\theta\\ 0 & s\phi & -c\phi s\theta\\ 1 & 0 & c\theta\end{pmatrix}\begin{pmatrix}\dot\phi\\ \dot\theta\\ \dot\psi\end{pmatrix} \tag{4}$$

The angular acceleration of the moving platform is obtained by differentiating (4)

$$\alpha=\begin{pmatrix}\alpha_X\\ \alpha_Y\\ \alpha_Z\end{pmatrix}=\begin{pmatrix}0 & c\phi & s\phi s\theta\\ 0 & s\phi & -c\phi s\theta\\ 1 & 0 & c\theta\end{pmatrix}\begin{pmatrix}\ddot\phi\\ \ddot\theta\\ \ddot\psi\end{pmatrix} + \begin{pmatrix}0 & -\dot\phi s\phi & \dot\phi c\phi s\theta+\dot\theta s\phi c\theta\\ 0 & \dot\phi c\phi & \dot\phi s\phi s\theta-\dot\theta c\phi c\theta\\ 0 & 0 & -\dot\theta s\theta\end{pmatrix}\begin{pmatrix}\dot\phi\\ \dot\theta\\ \dot\psi\end{pmatrix} \tag{5}$$

## 4. INVERSE KINEMATICS

The inverse kinematic problem of the Stewart Platform is concerned with the determination of the displacements of the six links and their time derivatives corresponding to a given Cartesian pose of the moving platform in terms of three positional displacements and three Euler angular displacements and their time derivatives. In the following sections, closed form solutions for the inverse position, rate and acceleration kinematics are presented.

### *4.1. Inverse position kinematics*

Referring back to Figure 1, the coordinates of the ith attachment point $a_i$ on the moving platform, given with reference to frame **P** as ${}^{P}\boldsymbol{a}_i=(x_{ai}, y_{ai}, z_{ai})^T$, are obtained with reference to the world coordinate system **W** by using

$$\boldsymbol{a}_i=\boldsymbol{x}+{}^{W}\boldsymbol{R}_P\,{}^{P}\boldsymbol{a}_i \tag{6}$$

Once the position of the attachment point $a_i$ is determined, the vector $\boldsymbol{L}_i$ of link $i$ is simply obtained as

$$\boldsymbol{L}_i=\boldsymbol{a}_i-\boldsymbol{b}_i \tag{7}$$

where $\boldsymbol{b}_i$ is a known 3-vector that represents the coordinates of the base attachment point $b_i$ with reference to frame **W**. The length $l_i$ of link $i$ will be simply computed from

$$l_i=\sqrt{\boldsymbol{L}_i\cdot\boldsymbol{L}_i} \tag{8}$$

Equations (6)–(8) represent the solution of the inverse position kinematic problem which involves determination of the six link lengths for a given Cartesian coordinate vector $\boldsymbol{q}$ representing the position and orientation of the moving platform. The unit vector along the axis of the prismatic joint of link $i$ is computed from

$$\boldsymbol{n}_i=\boldsymbol{L}_i/l_i \tag{9}$$

### *4.2. Inverse rate kinematics*

The velocity of point $a_i$ is obtained by differentiating Equation (6) with respect to time

$$\dot{\boldsymbol{a}}_i=\dot{\boldsymbol{x}}+\omega\times{}^{W}\boldsymbol{R}_P\,{}^{P}\boldsymbol{a}_i \tag{10}$$

The projection of this velocity vector on the axis of the prismatic joint of link $i$ yields the extension rate of link $i$

$$\dot l_i=\dot{\boldsymbol{a}}_i\cdot\boldsymbol{n}_i=\dot{\boldsymbol{x}}\cdot\boldsymbol{n}_i+\omega\times({}^{W}\boldsymbol{R}_P\,{}^{P}\boldsymbol{a}_i)\cdot\boldsymbol{n}_i \tag{11}$$

or

$$\dot l_i=\dot{\boldsymbol{x}}\cdot\boldsymbol{n}_i+\omega\cdot({}^{W}\boldsymbol{R}_P\,{}^{P}\boldsymbol{a}_i)\times\boldsymbol{n}_i \tag{12}$$

where, for a triple scalar product $\boldsymbol{a}\times\boldsymbol{b}\cdot\boldsymbol{c}$, the dot and cross products can be interchanged yielding $\boldsymbol{a}\cdot\boldsymbol{b}\times\boldsymbol{c}$, as long as the order of the vectors is not changed. For the purpose of deriving the inverse Jacobian matrix of the Stewart Platform, it is useful to write Equation (12) for the six links, in matrix form, as

$$\dot{\boldsymbol{l}}=\boldsymbol{J}_1^{-1}\begin{pmatrix}\dot{\boldsymbol{x}}\\ \omega\end{pmatrix} \tag{13}$$

where

$$\boldsymbol{J}_1^{-1}=\begin{pmatrix}\boldsymbol{n}_1^T & ({}^{W}\boldsymbol{R}_P\,{}^{P}\boldsymbol{a}_1\times\boldsymbol{n}_1)^T\\ \vdots & \vdots\\ \boldsymbol{n}_6^T & {}^{W}\boldsymbol{R}_P\,{}^{P}\boldsymbol{a}_6\times\boldsymbol{n}_6)^T\end{pmatrix} \tag{14}$$

Now substituting Equation (4) into Equation (13) yields

$$\dot{\boldsymbol{l}}=\boldsymbol{J}_1^{-1}\boldsymbol{J}_2^{-1}\dot{\boldsymbol{q}}=\boldsymbol{J}^{-1}\dot{\boldsymbol{q}} \tag{15}$$

where

$$\boldsymbol{J}_2^{-1}=\begin{pmatrix}\boldsymbol{I}_{3\times3} & & \boldsymbol{O}_{3\times3} & \\ & 0 & \cos\phi & \sin\phi\sin\theta\\ \boldsymbol{O}_{3\times3} & 0 & \sin\phi & -\cos\phi\sin\theta\\ & 1 & 0 & \cos\theta\end{pmatrix} \tag{16}$$

Equation (16) presents the solution to the inverse rate kinematic problem. $\boldsymbol{J}^{-1}=\boldsymbol{J}_1^{-1}\boldsymbol{J}_2^{-1}$ is the inverse Jacobian matrix of the machine.

The mechanism is in a singular position when $\det(\boldsymbol{J}^{-1})=0$. Such a condition will occur when either $\boldsymbol{J}_1^{-1}$ or $\boldsymbol{J}_2^{-1}$ are singular. The conditions for which $\boldsymbol{J}_1^{-1}$ is singular are difficult to find analytically for the general class of Stewart Platform mechanisms, since an analytical expression for the determinant of $\boldsymbol{J}_1^{-1}$ is not available. On the other hand, $\boldsymbol{J}_2^{-1}$ is singular for $\theta=0, \pi, \ldots, n\pi$. These two types of singularities are the configuration and formulation singularities respectively, as noted by Ma and Angeles.[12]

https://doi.org/10.1017/S0263574703005046 Published online by Cambridge University Press

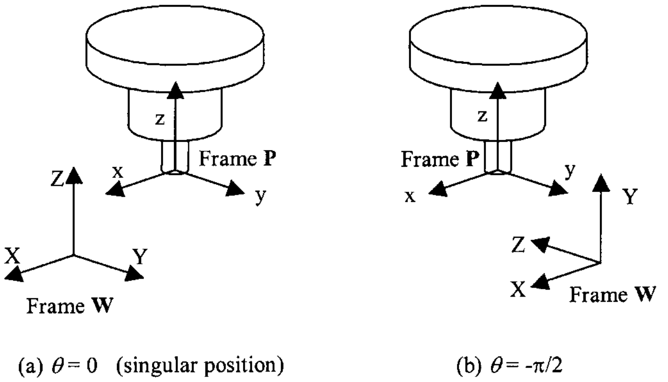


Fig. 3. Coordinate system assignments.

The formulation singularity is associated with the Euler angle formulation used. As we mentioned earlier, for the z-x-z Euler formulation, the formulation singularity will occur when $\boldsymbol{J}_2$ is singular or $\theta=0, \ldots, n\pi$. For the coordinate system assignment of Figure 3a, and the z-x-z Euler angle formulation, this type of singularity will occur for all horizontal positions of the platform. Since this situation can not be allowed in this application, this problem can be solved by either changing the Euler angle formulation or by changing the coordinate system assignment. The latter solution will be used here since the z-x-z Euler angle formulation enables us to directly identify the redundant orientation direction as discussed before. By changing the orientation of the fixed coordinate system **W**, as shown in Figure 3b, the formulation singularity will occur now when the platform is in a vertical position. This is far removed from normal operational configurations of the machine and will therefore not be encountered in practice.

### *4.3. Inverse acceleration kinematics*

The acceleration of point $a_i$ is obtained by differentiating Equation (10) with respect to time

$$\ddot{\boldsymbol{a}}_i=\ddot{x}+\alpha\times{}^W\boldsymbol{R}_P\,{}^P\boldsymbol{a}_i+\omega\times(\omega\times{}^W\boldsymbol{R}_P\,{}^P\boldsymbol{a}_i) \tag{17}$$

Now, $\ddot{l}_i$ is simply obtained by differentiating $\dot{\boldsymbol{l}}_i=\dot{\boldsymbol{a}}_i\cdot\boldsymbol{n}_i$ with respect to time

$$\ddot{l}_i=\ddot{\boldsymbol{a}}_i\cdot\boldsymbol{n}_i+\dot{\boldsymbol{a}}_i\cdot\dot{\boldsymbol{n}}_i \tag{18}$$

where $\dot{\boldsymbol{n}}_i$ is given by

$$\dot{\boldsymbol{n}}_i=\omega_i\times\boldsymbol{n}_i \tag{19}$$

where $\omega_i$ for $i=1, \ldots, 6$ are the angular velocities of the links, expressions for which will be derived in Section 6. It is possible to avoid computing $\omega_i$ for $i=1, \ldots, 6$, in order to evaluate Equation (19), since $\dot{\boldsymbol{n}}_i$ can also be determined by differentiating Equation (9) with respect to time, to obtain

$$\dot{\boldsymbol{n}}_i=(\boldsymbol{L}_i-\dot{l}_i\boldsymbol{n}_i)/l_i \tag{20}$$

Now, $l_i$ in Equation (20) is found by differentiating Equation (8) with respect to time which results in

$$\dot{l}_i=\frac{\boldsymbol{L}_i\cdot\dot{\boldsymbol{L}}_i}{l_i} \tag{21}$$

and $\dot{\boldsymbol{L}}_i$ is found by differentiating Equation (7) with respect to time and substituting Equation (10) to yield

$$\dot{\boldsymbol{L}}_i=\dot{x}+\omega\times{}^W\boldsymbol{R}_P\,{}^P\boldsymbol{a}_i \tag{22}$$

An alternative solution for the inverse acceleration kinematic problem in terms of the inverse Jacobian matrix is obtained by differentiating Equation (15) with respect to time

$$\ddot{l}=\boldsymbol{J}^{-1}\ddot{q}+\frac{d\boldsymbol{J}^{-1}}{dt}\dot{\boldsymbol{q}} \tag{23}$$

The time derivative of the inverse Jacobian matrix in Equation (23) is given by

$$\frac{d\boldsymbol{J}^{-1}}{dt}=\frac{d\boldsymbol{J}_1^{-1}}{dt}\boldsymbol{J}_2^{-1}+\boldsymbol{J}_1^{-1}\frac{d\boldsymbol{J}_2^{-1}}{dt} \tag{24}$$

where the time derivative matrices $\frac{d\boldsymbol{J}_1^{-1}}{dt}$ and $\frac{d\boldsymbol{J}_2^{-1}}{dt}$ are obtained by differentiating $\boldsymbol{J}_1^{-1}$ and $\boldsymbol{J}_2^{-1}$ with respect to time as

$$\frac{d\boldsymbol{J}_1^{-1}}{dt}=\begin{pmatrix}(\omega_1\times\boldsymbol{n}_1)^T & ((\omega\times{}^W\boldsymbol{R}_P\,{}^P\boldsymbol{a}_1)\times\boldsymbol{n}_1+{}^W\boldsymbol{R}_P\,{}^P\boldsymbol{a}_1\times(\omega_1\times\boldsymbol{n}_1))^T\\ \vdots & \vdots\\ (\omega_6\times\boldsymbol{n}_6)^T & ((\omega\times{}^W\boldsymbol{R}_P\,{}^P\boldsymbol{a}_6)\times\boldsymbol{n}_6+{}^W\boldsymbol{R}_P\,{}^P\boldsymbol{a}_6\times(\omega_6\times\boldsymbol{n}_6))^T\end{pmatrix} \tag{25}$$

$$\frac{d\boldsymbol{J}_2^{-1}}{dt}=\begin{pmatrix}\boldsymbol{O}_{3\times3} & & \boldsymbol{O}_{3\times3} & \\ & 0 & -\dot{\phi}s\phi & \dot{\phi}c\phi s\theta+\dot{\theta}s\phi c\theta\\ \boldsymbol{O}_{3\times3} & 0 & \dot{\phi}c\phi & \dot{\phi}s\phi s\theta-\dot{\theta}c\phi c\theta\\ & 0 & 0 & -\dot{\theta}s\theta\end{pmatrix} \tag{26}$$

Furthermore, we can replace $\omega_i\times\boldsymbol{n}_i$ by $\dot{\boldsymbol{n}}_i$ which can be computed from Equations (20)–(22).

## 5. FORWARD KINEMATICS

The forward kinematic problem can be stated as follows: For a given joint space coordinate vector $\boldsymbol{l}$, find the corresponding Cartesian coordinate vector $\boldsymbol{q}$. Unlike the inverse kinematic problem, the forward kinematic problem is much more difficult for the general class of Stewart Platforms. This is because there are many solutions, the number of solutions corresponding to the number of configurations the mechanism can be assembled into, for a given set of link lengths. The inverse kinematic solution represented by Equations (6)–(8) can not be inverted to find $\boldsymbol{q}$ for a given $\boldsymbol{l}$, since $\boldsymbol{q}$ does not occur explicitly in Equations (6)–(8). For the general class of Stewart Platforms, it has been shown that there are at most 40 possible solutions for the forward kinematic problem.[13,14] Only one solution, however, corresponds to the actual pose of a physical machine. A simple method that would take advantage of the availability of an estimate of this solution is needed.

In this section, we will evaluate the use of a numerical iterative technique, based on the Newton-Raphson method, to solve the forward kinematic problem. The Newton-Raphson method can be used to find the roots of single as well as multiple variable equations.[15] In the following, the presented procedure yields accurate results depending on the tolerance specified. This will be demonstrated by a numerical example.

https://doi.org/10.1017/S0263574703005046 Published online by Cambridge University Press

For a certain position of the mechanism, we will define a function $\boldsymbol{F}(\boldsymbol{q})$ as

$$\boldsymbol{F}(\boldsymbol{q}) = \boldsymbol{l}(\boldsymbol{q}) - \boldsymbol{l}_{given} \tag{27}$$

where $\boldsymbol{l}(\boldsymbol{q})$ is the joint space coordinate vector computed from the inverse kinematic solution using a Cartesian space coordinate vector $\boldsymbol{q}$, *and* $\boldsymbol{l}_{given}$ is the known joint space coordinate vector. If $\boldsymbol{q}$ is the required forward kinematic solution, $\boldsymbol{l}(\boldsymbol{q})$ will be equal to $\boldsymbol{l}_{given}$, and $\boldsymbol{F}(\boldsymbol{q})$ will be zero. A numerical solution using the Newton-Raphson method is given by

$$\tilde{\boldsymbol{q}}_i = \tilde{\boldsymbol{q}}_{i-1} - \left(\frac{\partial \boldsymbol{F}(\tilde{\boldsymbol{q}}_{i-1})}{\partial \boldsymbol{q}}\right)^{-1} \boldsymbol{F}(\tilde{\boldsymbol{q}}_{i-1}) \tag{28}$$

where $\tilde{\boldsymbol{q}}_i$ is the approximate solution obtained after the ith iteration. It can be shown that the matrix $\frac{\partial \boldsymbol{F}(\tilde{\boldsymbol{q}}_{i-1})}{\partial \boldsymbol{q}}$ is same as the inverse Jacobian matrix $\boldsymbol{J}^{-1}(\tilde{\boldsymbol{q}}_{i-1})$ given by Equation (15). Hence, Equation (28) may be written as

$$\tilde{\boldsymbol{q}}_i = \tilde{\boldsymbol{q}}_{i-1} - \boldsymbol{J}(\tilde{\boldsymbol{q}}_{i-1})(\boldsymbol{l}(\tilde{\boldsymbol{q}}_{i-1}) - \boldsymbol{l}_{given}) \tag{29}$$

Starting with an initial guess $\tilde{\boldsymbol{q}}_O$, Equation (29) is used in an iterative fashion until an acceptable solution is reached. Since there are many solutions, it is very important to start with an initial guess close to the actual pose of the platform. Such an initial guess could be either the known desired Cartesian pose, or the pose of a previous point on the trajectory a short time interval in the past.

**Numerical Example:** In this example, a computer program is written to implement the Newton-Raphson procedure developed. For the kinematic parameters of the Stewart Platform based machining center in Tables I and II, let the platform be in the Cartesian pose

$$\boldsymbol{q} = (0.2, 0.3, -0.4, 0.1, -1.4, 0.1)^T \tag{30}$$

where the linear displacements are stated in meters and the angular displacements are in radians. The inverse position kinematics computations result in a joint space coordinate vector

$$\boldsymbol{l} = (3.0508, 3.2324, 3.2997, 3.4560, 3.5797, 3.6935)^T \tag{31}$$

where all the joint lengths are stated in meters. We assume now that $\boldsymbol{l}$ is given by Equation (31), presumably from joint space measurements, and that we need to find an approximate numerical solution for $\boldsymbol{q}$. Applying the numerical technique presented in this section with an initial guess

$$\boldsymbol{q}_O = (0.25, 0.25, -0.45, 0.07, -1.7, 0.07)^T \tag{32}$$

and a tolerance of $1 \times 10^{-6}$ as the stopping criterion, convergence is reached after three iterations as shown in Table III.

## 6. KINEMATICS OF THE LINKS AND JOINTS

Before proceeding to the dynamics of the Stewart Platform mechanism, we need first to determine expressions for the link angular velocities and accelerations. These expressions, together with expressions for the link extension rates and accelerations, are needed for the development of the rigid body dynamic equations subsequently in the paper. Unlike the link extension rates and accelerations, the angular velocities and accelerations of the links depend on the specific types of the joints at the two ends of the struts. We will assume first that the struts are attached to the platform

Table I. Attachment points on the moving platform with reference to Frame **P**.

| | $a_1$(m) | $a_2$(m) | $a_3$(m) | $a_4$(m) | $a_5$(m) | $a_6$(m) |
|---|---|---|---|---|---|---|
| $x$ | 0.225 | 0.1125 | –0.1125 | –0.225 | –0.1125 | 0.1125 |
| $y$ | 0.0 | 0.1949 | 0.1949 | 0.0 | –0.1949 | –0.1949 |
| $z$ | –0.228 | –0.228 | –0.228 | –0.228 | –0.228 | –0.228 |

Table II. Attachment points on the base with reference to Frame **W**.

| | $b_1$(m) | $b_2$(m) | $b_3$(m) | $b_4$(m) | $b_5$(m) | $b_6$(m) |
|---|---|---|---|---|---|---|
| $X$ | 1.7580 | 1.6021 | –1.7580 | –1.6021 | 0.0 | 0.0 |
| $Y$ | 2.8 | 3.07 | 2.8 | 3.07 | 2.8 | 3.07 |
| $Z$ | –1.015 | –0.925 | –1.015 | –0.925 | 2.03 | 1.85 |

Table III. Results of using Newton-Raphson method to solve the forward kinematic problem.

| | $X$(m) | $Y$(m) | $Z$(m) | $\phi$(rad) | $\theta$(rad) | $\psi$(rad) |
|---|---|---|---|---|---|---|
| 0 | 0.25 | 0.25 | –0.45 | 0.07 | –1.7 | 0.07 |
| 1 | 0.1933094 | 0.3077386 | –0.4089530 | 0.1126940 | –1.404225 | 0.1023974 |
| 2 | 0.2000163 | 0.2999979 | –0.4000039 | 0.0999466 | –1.400029 | 0.0999672 |
| 3 | 0.2000000 | 0.3000000 | –0.4000000 | 0.1000000 | –1.400000 | 0.1000000 |

https://doi.org/10.1017/S0263574703005046 Published online by Cambridge University Press

through three degree-of-freedom spherical joints, and to the base through two degree-offreedom universal joints.

For a given motion of the moving platform, the motions of the attachments points of the links to the platform can be determined as discussed in the previous sections. $\boldsymbol{a}_i$, $\dot{\boldsymbol{a}}_i$ and $\ddot{\boldsymbol{a}}_i$ for point $a_i$ are computed from Equations (6), (10) and (17), respectively, for a known platform Cartesian position, velocity and acceleration vectors. On the other hand, $\boldsymbol{a}_i$, $\dot{\boldsymbol{a}}_i$ and $\ddot{\boldsymbol{a}}_i$ can also be written in term of the motion of link $i$. First, $\boldsymbol{a}_i$ is given by

$$\boldsymbol{a}_i = l_i\,\boldsymbol{n}_i + \boldsymbol{b}_i \tag{33}$$

By differentiating Equation (33) with respect to time, we get $\dot{\boldsymbol{a}}_i$ as

$$\dot{\boldsymbol{a}}_i = \omega_i \times l_i\,\boldsymbol{n}_i + \dot{l}_i\,\boldsymbol{n}_i \tag{34}$$

where the $\omega_i$ is the angular velocity of the link $i$ and will be defined shortly. By differentiating Equation (34) with respect to time, we get $\ddot{\boldsymbol{a}}_i$ as

$$\ddot{\boldsymbol{a}}_i = \alpha_i \times l_i\,\boldsymbol{n}_i + \omega_i \times (\omega_i \times l_i\,\boldsymbol{n}_i) + 2\omega_i \times \dot{l}_i\,\boldsymbol{n}_i + \ddot{l}_i\,\boldsymbol{n}_i \tag{35}$$

where $\alpha_i$ is angular acceleration of link $i$.

The extension rate of the $i$th link is simply obtained by taking the dot product of the two sides of Equation (34) with $\boldsymbol{n}_i$, which yields

$$\dot{l}_i = \dot{\boldsymbol{a}}_i \cdot \boldsymbol{n}_i \tag{36}$$

However, even with knowledge of $\dot{l}_i$, we still cannot solve Equation (34) for $\omega_i$ since the $3\times3$ system of linear equations that results from expanding Equation (34) is not full rank. In some references,[7,8] the relation $\omega_i \cdot \boldsymbol{n}_i = 0$ is used, which is an approximation and true only at the instant when $\boldsymbol{n}_i$ is normal to the fixed axis of the universal joint. An exact solution can be obtained by explicitly considering the kinematic model of the universal joint.

Figure 4 shows a typical Stewart Platform strut with a 2 degree-of-freedom universal joint at the base attachment point, and a 3 degree-of-freedom spherical joint at the platform attachment point. The unit vector $\boldsymbol{u}_i$ along the axis of the fixed revolute joint of the universal joint is determined from the geometry of the mechanism. The unit vector $\boldsymbol{v}_i$ along the axis of the other revolute joint rotates in a plane normal to $\boldsymbol{u}_i$, and since it is also normal to $\boldsymbol{n}_i$, it is simply computed from

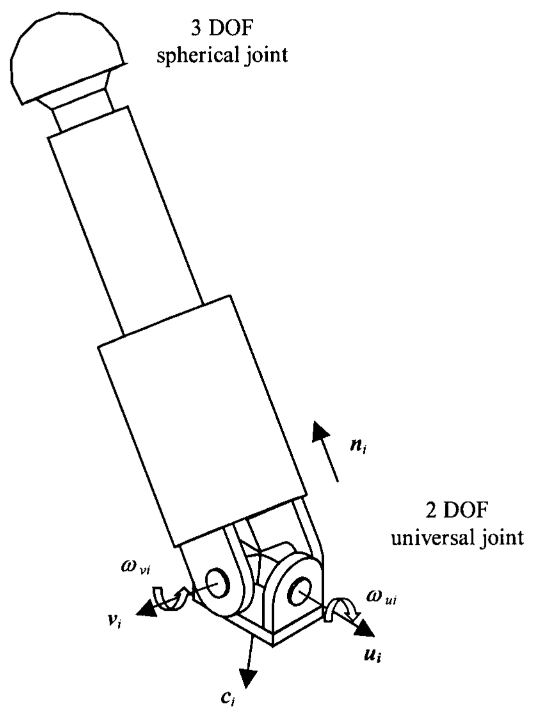


Fig. 4. A Stewart platform strut.

$$\boldsymbol{v}_i = \frac{\boldsymbol{u}_i \times \boldsymbol{n}_i}{\|\boldsymbol{u}_i \times \boldsymbol{n}_i\|} \tag{37}$$

The angular velocity $\omega_i$ of link $i$ can be resolved into two components along the revolute joint axes $\boldsymbol{u}_i$ and $\boldsymbol{v}_i$ of the universal joint, and therefore we can write

$$\omega_i = \omega_{ui}\,\boldsymbol{u}_\mathrm{i} + \omega_{vi}\,\boldsymbol{v}_\mathrm{i} \tag{38}$$

The magnitudes of these two components can be obtained by substituting Equation (38) into Equation (34), and taking the dot product of the two sides of the resulting equation with $\boldsymbol{v}_i$ to solve for $\omega_{ui}$ and with $\boldsymbol{u}_i$ to solve for $\omega_{vi}$

$$\omega_{ui} = -(\dot{\boldsymbol{a}}_i - \dot{l}_i\,\boldsymbol{n}_i) \cdot \boldsymbol{v}_i / (l_i\,\boldsymbol{n}_i \cdot \boldsymbol{c}_i) \tag{39}$$

$$\omega_{vi} = (\dot{\boldsymbol{a}}_i - \dot{l}_i\,\boldsymbol{n}_i) \cdot \boldsymbol{u}_i / (l_i\,\boldsymbol{n}_i \cdot \boldsymbol{c}_i) \tag{40}$$

where $\boldsymbol{c}_i$ is defined as

$$\boldsymbol{c}_i = \boldsymbol{u}_i \times \boldsymbol{v}_i \tag{41}$$

Link $i$ has zero angular velocity component along the direction of $\boldsymbol{c}_i$, since it is always normal to the two axes of rotation of link $i$, $\boldsymbol{u}_i$ and $\boldsymbol{v}_i$.

The acceleration of point $a_i$ is given in terms of the variables related to the motion of link $i$ by Equation (35). Taking the dot product of both sides with $\boldsymbol{n}_i$, we get the extensional acceleration of link $i$ as

$$\ddot{l}_i = \ddot{\boldsymbol{a}}_i \cdot \boldsymbol{n}_i - l_i(\omega_i \times (\omega_i \times \boldsymbol{n}_i)) \cdot \boldsymbol{n}_i \tag{42}$$

As before, even with the knowledge of $\ddot{l}_i$, we still can not solve the linear system of Equations (35) for $\alpha_i$, and we would again need to use the universal joint kinematic model. Differentiating Equation (38) with respect to time, we get

$$\alpha_i = \alpha_{ui}\,\boldsymbol{u}_\mathrm{i} + \alpha_{vi}\,\boldsymbol{v}_\mathrm{i} + \omega_{ui}\,\omega_{vi}\,\boldsymbol{c}_\mathrm{i} \tag{43}$$

In the last equation, we used $\dot{\boldsymbol{u}}_i = 0$ and $\dot{\boldsymbol{v}}_i = \omega_{ui}\,\boldsymbol{u}_i \times \boldsymbol{v}_i$, which is obtained from the fact that the position vector $\boldsymbol{v}_i$ is rotating with an angular velocity of $\omega_{ui}\,\boldsymbol{n}_i$. Substituting Equation (43) into Equation (35) will yield

$$\alpha_{ui} = -\ddot{\boldsymbol{a}}_i' \cdot \boldsymbol{v}_i / (l_i\,\boldsymbol{n}_i \cdot \boldsymbol{c}_i) \tag{44}$$

$$\alpha_{vi} = \ddot{\boldsymbol{a}}_i' \cdot \boldsymbol{u}_i / (l_i\,\boldsymbol{n}_i \cdot \boldsymbol{c}_i) \tag{45}$$

where

$$\ddot{\boldsymbol{a}}_i' = \ddot{\boldsymbol{a}}_i - \omega_{ui}\,\omega_{vi}\,l_i\,\boldsymbol{c}_i \times \boldsymbol{n}_i - \ddot{l}_i\,\boldsymbol{n}_i - 2\,\dot{l}_i\,\omega_i \times \boldsymbol{n}_i - l_i\,\omega_i \times (\omega_i \times \boldsymbol{n}_i) \tag{46}$$

In the previous analysis in this section, we assumed that a 2 degree-of-freedom universal joint is used at the base end and a 3 degree-of-freedom spherical joint is used at the moving platform end. If, instead, the spherical joint is used at the base end and the universal joint is used at the platform end, the derivation for the angular velocities and accelera-

https://doi.org/10.1017/S0263574703005046 Published online by Cambridge University Press

tions of the links will be slightly different. For the angular velocity, the previous procedure can be used to determine $\dot{l}_i$, $\omega_{ui}$, and $\omega_{vi}$. However, in this case, we should compute $\boldsymbol{u}_i$ from $\boldsymbol{u}_i = {}^W\boldsymbol{R}_P\,{}^P\boldsymbol{u}_i$ where ${}^P\boldsymbol{u}_i$ is the unit vector of the revolute joint fixed to the platform and is given with reference to frame **P**. In addition to the two velocity components of Equation (38), a third angular velocity component will be transmitted from the platform to link $i$ through the 2 degree-of-freedom joint along the $\boldsymbol{c}_i$ direction. Therefore, the angular velocity of link $i$ should be written for this case as

$$\omega_i = \omega_{ui}\,\boldsymbol{u}_i + \omega_{vi}\,\boldsymbol{v}_i + (\omega \cdot \boldsymbol{c}_i)\boldsymbol{c}_i \tag{47}$$

For the angular acceleration, we can use the same procedure. However, the equation corresponding to Equation (43) will have more terms which come from differentiating Equation (47) with respect to time. In particular, note that $\dot{\boldsymbol{u}}_i$ is not zero, and neither is $\dot{\boldsymbol{c}}_i$.

Taking into consideration these details, the angular acceleration of link $i$ can be obtained for this case as

$$\alpha_i = \alpha_{ui}\,\boldsymbol{u}_i + \alpha_{vi}\,\boldsymbol{v}_i + (\alpha \cdot \boldsymbol{c}_i)\boldsymbol{c}_i + \omega_{ui}\omega_{vi}\boldsymbol{c}_i - 2\omega_{ui}(\omega \cdot \boldsymbol{v}_i)\boldsymbol{c}_i - \omega_{vi}(\omega \cdot \boldsymbol{c}_i)\boldsymbol{u}_i + (\omega \cdot \boldsymbol{v}_i)(\omega \cdot \boldsymbol{u}_i)\boldsymbol{c}_i + (\omega \cdot \boldsymbol{c}_i)(\omega \cdot \boldsymbol{v}_i)\boldsymbol{u}_i \tag{48}$$

Finally, if two spherical joints are used at the two ends of the links, kinematic redundancy results. Hence, exact values for the angular velocities and accelerations of the links are not obtainable from kinematic considerations alone. For the case of an electromechanically actuated strut with spherical joints at both ends, shown in Figure 5, electromagnetic torque generated at the motor rotates the rotor in one direction while an equal reaction torque will be exerted on the stator in the opposite direction. The electromagnetic torque on the rotor will be transmitted to the ballscrew and to the nut. Since the nut and the attached inner strut tube are constrained from rotation, the torque transmitted to the nut will in turn be transmitted to the outer strut tube, to which the motor stator is fixed, and therefore will cancel the reaction torque on the stator. However, due to friction losses in the transmission, these two opposing torque components may not be exactly equal in magnitude. Therefore, a small differential torque may result on the outer tube of the strut, which could rotate the whole strut about its axis. This rotation will be opposed only by the friction in the two spherical joints. This rotation of the strut, however, will not affect the relative motion between the screw and the nut which will result in the extension (or retraction) of the link. In an early version of the Ingersoll Octahedral Hexapod, springs connecting each pair of struts near the base joints are used to help the spherical joint friction in preventing strut rotation. It has been observed that the struts do rotate by small amounts for some maneuvers, and the restraining springs are exercised. If this behavior is to be modeled, models of spherical joint friction will have to be added along with models of frictional losses in the ballscrew drive and the spring force-deflection characteristics.

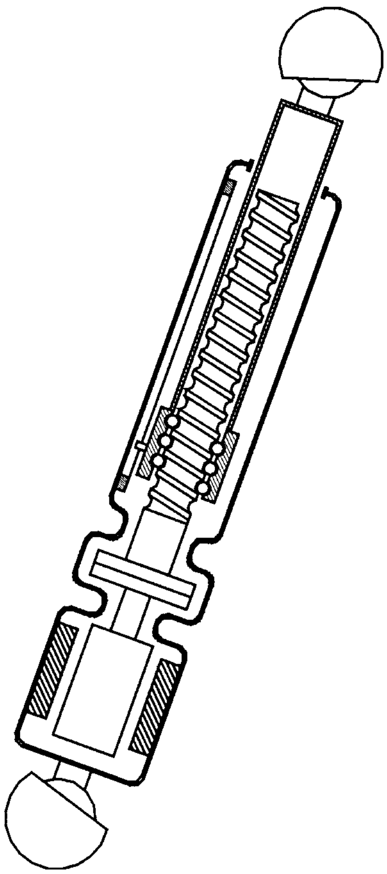

Fig. 5. Electromechanically actuated strut with spherical joint at both ends.

A simplifying approximation, in the case of the last design, is to assume that there is no rotation about the axial direction which implies that $\omega_i$ is perpendicular to $\boldsymbol{n}_i$. This assumption will greatly simplify the kinematic equations for the angular velocity and acceleration of the strut. By taking the cross product with $\boldsymbol{n}_i$ on both sides of Equations (34) and (35) and simplifying using the above assumption, we get

$$\omega_i = (\boldsymbol{n}_i \times \dot{\boldsymbol{a}}_i)/l_i \tag{49}$$

$$\alpha_i = (\boldsymbol{n}_i \times \ddot{\boldsymbol{a}}_i - 2\dot{l}_i\,\omega_i)/l_i \tag{50}$$

## 7. INVERSE DYNAMIC EQUATIONS

The recursive Newton-Euler formulation requires that all the necessary kinematic variables, which include the platform variables $\omega$ and $\alpha$ and the strut variables $l_i$, $\dot{l}_i$, $\ddot{l}_i$, $n_i$, $\omega_i$ and $\alpha_i$ be stated in terms of a given generalized coordinate vector $\boldsymbol{q}$ and its first and second time derivatives. This procedure is discussed in detail in the previous sections. In addition, we need to determine the acceleration vectors $\boldsymbol{a}_{i1}$, $\boldsymbol{a}_{i2}$ of the centers of mass of the moving and stationary parts 1 and 2 of link $i$. Part 1, the moving part, includes all the components that translate axially in addition to the rotational motion of the strut. For the case of an electromechanical strut, Part 1 includes the nut and the output shaft, whereas Part 2, the stationary part, includes all the remaining components that only rotate. The accelerations of the centers of mass of parts 1 and 2 are given by

$$\boldsymbol{a}_{i1} = (l_i - l_1)\omega_i \times (\omega_i \times \boldsymbol{n}_i) + (l_i - l_1)\alpha_i \times \boldsymbol{n}_i + 2\omega_i \times \dot{l}_i\,\boldsymbol{n}_i + \ddot{l}_i\,\boldsymbol{n}_i \tag{51}$$

$$\boldsymbol{a}_{i2} = l_2\,\omega_i \times (\omega_i \times \boldsymbol{n}_i) + l_2\,\alpha_i \times \boldsymbol{n}_i \tag{52}$$

where $l_1$ and $l_2$ are the lengths between the centers of mass of parts 1 and 2 and the attachment points $a_i$ and $b_i$, respectively, as shown in Figure 6.

https://doi.org/10.1017/S0263574703005046 Published online by Cambridge University Press

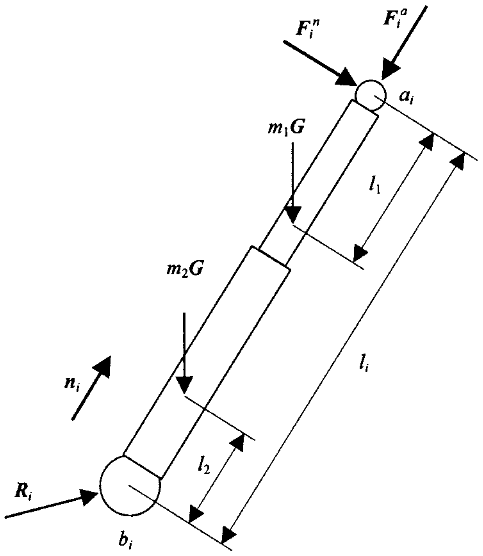


Fig. 6. Force components on link $i$ for the case of two frictionless spherical joints.

With all the needed kinematic information available, we can proceed to determine the dynamic equations of the system by finding the reaction forces between the links and the moving platform first. Let the reaction force of the platform acting on link $i$ be resolved into two components, as shown in Figure 6, one component $\boldsymbol{F}_i^a$ along the prismatic joint axis of link $i$, and the other component $\boldsymbol{F}_i^n$ normal to the joint axis.[7]

$$\boldsymbol{F}_i = \boldsymbol{F}_i^a + \boldsymbol{F}_i^n \tag{53}$$

Now, assuming a 2 degree-of-freedom universal joint is used either at the base joint or at the platform joint, a moment component about an axis normal to the axes of the two revolute joints of the universal joint will be transmitted to link $i$ from the base or the platform. This reaction moment on the link $i$ can be written as

$$\boldsymbol{M}_i = m_i \boldsymbol{c}_i \tag{54}$$

where $\boldsymbol{c}_i$ is a unit vector normal to the two axes of the universal joint as previously defined, and $m_i$ is the magnitude of this reaction moment. Link $i$ will also be subjected to gravitational force components $m_1\boldsymbol{G}$ and $m_2\boldsymbol{G}$ at the centers of mass of the moving and stationary parts 1 and 2, respectively, where $\boldsymbol{G}=(0,\ -g,\ 0)^T$ and $g$ is the acceleration due to gravity. The gravity field here is in the negative Y direction since the Y-axis of the world coordinate system **W** is chosen to be vertical to avoid the formulation singularity problem associated with the chosen Euler angles when the moving platform is horizontal.

Having established all the external force and moment components on link $i$, balancing the moment components about the base joint gives

$$m_1(l_i - l_1)\boldsymbol{n}_i \times \boldsymbol{G} + m_2 l_2\, \boldsymbol{n}_i \times \boldsymbol{G} + l_i\, \boldsymbol{n}_i \times \boldsymbol{F}_i^n + \boldsymbol{M}_i$$
$$= (\bar{\boldsymbol{I}}_1 + \bar{\boldsymbol{I}}_2)\alpha_i - (\bar{\boldsymbol{I}}_1 + \bar{\boldsymbol{I}}_2)\omega_i \times \omega_i + m_1(l_i - l_1)\boldsymbol{n}_i \times \boldsymbol{a}_{i1} + m_2 l_2 \boldsymbol{n}_i \times \boldsymbol{a}_{i2} \tag{55}$$

where $\bar{\boldsymbol{I}}_1$, and $\bar{\boldsymbol{I}}_2$ are the mass moments of inertia tensors of parts 1 and 2 respectively, with reference to the world coordinate system **W** and at the centers of mass of the two parts. The moment components on the left hand side of Equation (55) are due to the gravitational forces on parts 1 and 2, the normal force component at joint $a_i$, and the reaction moment at the universal joint either at $a_i$ or $b_i$. These components balance the inertial moment components shown on the right hand side of Equation (55). By using Equation (54), Equation (55) can be written compactly as

$$l_i\, \boldsymbol{n}_i \times \boldsymbol{F}_i^n + m_i \boldsymbol{c}_i = \boldsymbol{N}_i \tag{56}$$

where $\boldsymbol{N}_i$ can be evaluated from

$$\boldsymbol{N}_i = -m_1(l_i - l_1)\boldsymbol{n}_i \times \boldsymbol{G} - m_2 l_2\, \boldsymbol{n}_i \times \boldsymbol{G} + (\bar{\boldsymbol{I}}_1 + \bar{\boldsymbol{I}}_2)\alpha_i$$
$$- (\bar{\boldsymbol{I}}_1 + \bar{\boldsymbol{I}}_2)\omega_i \times \omega_i + m_1(l_i - l_1)\boldsymbol{n}_i \times \boldsymbol{a}_{i1} + m_2 l_2\, \boldsymbol{n}_i \times \boldsymbol{a}_{i2} \tag{57}$$

For axisymmetric links, we can avoid computing the inertia tensors $\bar{\boldsymbol{I}}_1$ and $\bar{\boldsymbol{I}}_2$ in Equation (57) by substituting the following relations which involve the scalar quantities $\bar{I}_{aa1}$, $\bar{I}_{aa2}$, $\bar{I}_{nn1}$, and $\bar{I}_{nn2}$ representing the mass moments of inertia along the axial and normal directions of the links for parts 1 and 2 at the respective centers of mass.[16] Details are given in the Appendix.

$$(\bar{\boldsymbol{I}}_1 + \bar{\boldsymbol{I}}_2)\alpha_i = (\bar{I}_{aa1} + \bar{I}_{aa2})(\alpha_i \cdot \boldsymbol{n}_i)\boldsymbol{n}_i + (\bar{I}_{nn1} + \bar{I}_{nn2})\boldsymbol{n}_i \times (\alpha_i \times \boldsymbol{n}_i) \tag{58}$$

$$(\bar{\boldsymbol{I}}_1 + \bar{\boldsymbol{I}}_2)\omega_\mathrm{i} \times \omega_\mathrm{i} = (\bar{I}_{aa1} + \bar{I}_{aa2} - \bar{I}_{nn1} - \bar{I}_{nn2})(\omega_\mathrm{i} \cdot \boldsymbol{n}_i)\boldsymbol{n}_i \times \omega_\mathrm{i} \tag{59}$$

Taking the dot product of both sides of Equation (56) with $\boldsymbol{n}_i$, the term containing $\boldsymbol{F}_i^n$ will drop out since it is normal to $\boldsymbol{n}_i$, and $m_i$ can be determined as

$$m_i = (\boldsymbol{N}_i \cdot \boldsymbol{n}_i)/(\boldsymbol{c}_i \cdot \boldsymbol{n}_i) \tag{60}$$

There is no solution for $m_i$ if $\boldsymbol{c}_i$ is perpendicular to $\boldsymbol{n}_i$, which would only occur if the strut axis coincides with the axis of the fixed revolute joint. With proper design this position can be avoided. If spherical joints are used at both ends of the strut, $m_i$ will be zero. Once $m_i$ is determined, it can be substituted into Equation (56) to get $\boldsymbol{F}_i^n$ from

$$\boldsymbol{F}_i^n = (\boldsymbol{N}_i \times \boldsymbol{n}_i - m_i \boldsymbol{c}_i \times \boldsymbol{n}_i)/l_i \tag{61}$$

For the case of frictionless spherical joints at both strut ends, Equation (61) can be used, the term containing $m_i$ being zero. For this case also, and referring to Equations (58) and (59), only the term $(\bar{I}_{nn1} + \bar{I}_{nn2})\alpha_i \times \boldsymbol{n}_i$ will be nonzero, among all the terms in Equations (58) and (59), since $\omega_i \cdot \boldsymbol{n}_i = 0$ and $\alpha_i \cdot \boldsymbol{n}_i = 0$. Therefore, only the moment of inertia components $\bar{I}_{nn1}$ and $\bar{I}_{nn2}$ will be needed in the equations if frictionless spherical joints are used at both ends of each strut. Hence, the net inertial moment component along the axial direction is zero for this case. This is consistent with our assumption that frictionless spherical joints do not transmit moments and hence there is no axial rotation of the struts.

Once we have determined the normal force component $\boldsymbol{F}_i^n$ and the reaction moment $\boldsymbol{M}_i$ transmitted through the universal joint, we can proceed to find the axial force component $\boldsymbol{F}_i^a$. We take advantage of the fact that the line of action of this force is along the prismatic joint axis of link $i$ and therefore we can write $\boldsymbol{F}_i^a$ in the form

$$\boldsymbol{F}_i^a = f_i^a\, \boldsymbol{n}_i \tag{62}$$

where $f_i^a$ contains the magnitude and sign of $\boldsymbol{F}_i^a$. The six scalar quantities $f_i^a$ for $i = 1, \ldots, 6$ can be determined from the summation of the force and moment components acting on the platform which will result in

https://doi.org/10.1017/S0263574703005046 Published online by Cambridge University Press

$$-\sum_{i=1}^{6} f_i^a \boldsymbol{n}_i - \sum_{i=1}^{6} \boldsymbol{F}_i^n + m_p \boldsymbol{G} = m_p \ddot{\boldsymbol{x}}_g \tag{63}$$

and

$$m_p \bar{\boldsymbol{r}} \times \boldsymbol{G} - \sum_{i=1}^{6} f_i^a \, {}^W\boldsymbol{R}_P \, {}^P\boldsymbol{a}_i \times \boldsymbol{n}_i - \sum_{i=1}^{6} {}^W\boldsymbol{R}_P \, {}^P\boldsymbol{a}_i \times \boldsymbol{F}_i^n - \sum_{i=1}^{6} \boldsymbol{M}_i$$

$$= \bar{\boldsymbol{I}}_P \alpha - \bar{\boldsymbol{I}}_P \omega \times \omega + m_p (\bar{\boldsymbol{r}} \times \ddot{\boldsymbol{x}}_g) \tag{64}$$

where $m_p$ is the mass of the platform. $\ddot{\boldsymbol{x}}_g$ is the acceleration of the platform center of mass, which is determined in terms of the platform motion variables as

$$\ddot{\boldsymbol{x}}_g = \ddot{\boldsymbol{x}} + \alpha \times \bar{\boldsymbol{r}} + \omega \times (\omega \times \bar{\boldsymbol{r}}) \tag{65}$$

and

$$\bar{\boldsymbol{r}} = {}^w\boldsymbol{R}_p \, {}^p\bar{\boldsymbol{r}} \tag{66}$$

where ${}^P\bar{\boldsymbol{r}}$ is the 3-vector of the center of mass of the platform with reference to the frame **P**. Also, the mass moments of inertia of the platform $\bar{\boldsymbol{I}}_p$ with reference to the world frame **W** at the center of mass of the platform, in Equation (64), is time varying due to the rotation of the platform. It can be related to the constant mass moments of inertia of the platform ${}^P\bar{\boldsymbol{I}}_p$ described with reference to frame **P** by the following relation.[16] Details are given in the Appendix.

$$\bar{\boldsymbol{I}}_p = {}^w\boldsymbol{R}_p \, {}^P\bar{\boldsymbol{I}}_p \, {}^w\boldsymbol{R}_p^T \tag{67}$$

Equations (63) and (64) make a system of 6 linear equations in $f_i^a$ for $i = 1, \ldots, 6$. They can be solved for $f_i^a$ as

$$\begin{pmatrix} f_1^a \\ \vdots \\ f_6^a \end{pmatrix} = \boldsymbol{J}_1^T \boldsymbol{C} \tag{68}$$

where we use the matrix $\boldsymbol{J}_1^{-1}$ as given by Equation (14), and define the known vector $\boldsymbol{C}$ as

$$\boldsymbol{C} = \left\{ \begin{matrix} m_P \boldsymbol{G} - m_P \ddot{\boldsymbol{x}}_g - \sum_{i=1}^{6} \boldsymbol{F}_i^n \\ m_P \bar{\boldsymbol{r}} \times \boldsymbol{G} - m_p (\bar{\boldsymbol{r}} \times \ddot{\boldsymbol{x}}_g) - \bar{\boldsymbol{I}}_P \alpha + \bar{\boldsymbol{I}}_P \omega \times \omega - \sum_{i=1}^{6} {}^W\boldsymbol{R}_P \, {}^P\boldsymbol{a}_i \times \boldsymbol{F}_i^n - \sum_{i=1}^{6} \boldsymbol{M}_i \end{matrix} \right\} \tag{69}$$

Note that, for a configuration with a universal joint at the base end, the reaction moment $\boldsymbol{M}_i$ is transferred from the base to the strut. Therefore, the term $\sum_{i=1}^{6} \boldsymbol{M}_i$ should not be present in Equations (64) and (69) if a spherical joint is used at the platform end. We see from Equation (68) that the solution requires inverting the $6 \times 6$ matrix $\boldsymbol{J}_1^{-1}$, which can only be done numerically since an analytical solution for inverting $\boldsymbol{J}_1^{-1}$ is not available.

Once the interaction forces between the struts and the moving platform are determined, we proceed to compute the actuation forces $f_i$ that power the prismatic joints. This force component will be the axial force that the ball screw exerts on the nut for the electromechanical actuation considered. $f_i$ is determined by summing the axial force components acting on the inner strut tube and nut (part 1), which results in

$$f_i = m_1 \boldsymbol{a}_{i1} \cdot \boldsymbol{n}_i - f_i^a - m_1 \boldsymbol{G} \cdot \boldsymbol{n}_i \tag{70}$$

The joint space force vector $\boldsymbol{F}$, containing the six actuation force components $f_i$ for $i = 1 \ldots 6$, can be written as

$$\boldsymbol{F} = (f_1 \ldots f_6)^T \tag{71}$$

Using Equation (70), $\boldsymbol{F}$ can be obtained as

$$\boldsymbol{F} = \begin{pmatrix} m_1(\boldsymbol{a}_{11} - \boldsymbol{G}) \cdot \boldsymbol{n}_1 \\ \vdots \\ m_1(\boldsymbol{a}_{61} - \boldsymbol{G}) \cdot \boldsymbol{n}_6 \end{pmatrix} - \boldsymbol{J}_1^T \boldsymbol{C} \tag{72}$$

On the other hand, the Cartesian space force/torque vector

$$\tau = (f_x \; f_y \; f_z \; \tau_\phi \; \tau_\theta \; \tau_\psi)^T \tag{73}$$

can be obtained using the Jacobian matrix $\boldsymbol{J}$.

$$\tau = \boldsymbol{J}^{-T} \boldsymbol{F} \tag{74}$$

or

$$\tau = \boldsymbol{J}^{-T} \begin{pmatrix} m_1(\boldsymbol{a}_{11} - \boldsymbol{G}) \cdot \boldsymbol{n}_1 \\ \vdots \\ m_1(\boldsymbol{a}_{61} - \boldsymbol{G}) \cdot \boldsymbol{n}_6 \end{pmatrix} - \boldsymbol{J}_2^{-T} \boldsymbol{C} \tag{75}$$

where $\boldsymbol{J}_2^{-T}$ is given by Equation (16). Equation (75) represents a closed form solution of the inverse dynamics of the Stewart platform mechanism in Cartesian coordinates. The solution does not require inverting any matrix since the Jacobian matrix is derived in its inverse form.

## 8. FORWARD DYNAMICS

The inverse dynamic problem for Stewart Platform mechanisms can be stated as: given the generalized position, velocity and acceleration vectors, find the corresponding force/torque vector that results in such motion. On the other hand, the forward dynamic problem can be stated as: given the input force/torque vector, find the corresponding motion in terms of Cartesian position, velocity and acceleration for some initial position and velocity conditions.

In contrast to the Lagrangian formulation, the Newton-Euler formulation can not be directly used to obtain a closed form forward dynamic solution in which the generalized acceleration vector $\ddot{\boldsymbol{q}}$ is separated. For the purpose of simulating the dynamics of Stewart Platform mechanisms, however, the derived dynamic equations need to be put in the form

$$\tau = \boldsymbol{M}(\boldsymbol{q})\ddot{\boldsymbol{q}} + \boldsymbol{N}(\boldsymbol{q}, \dot{\boldsymbol{q}}) + \boldsymbol{G}(\boldsymbol{q}) \tag{76}$$

where

$\boldsymbol{M}(\boldsymbol{q})$ is the inertia matrix of the machine.
$\boldsymbol{N}(\boldsymbol{q}, \dot{\boldsymbol{q}})$ contains the Coriolis and centrifugal force/torque components.
$\boldsymbol{G}(\boldsymbol{q})$ contains the gravity force/torque components.

Setting $\boldsymbol{h}(\boldsymbol{q}, \dot{\boldsymbol{q}}) = \boldsymbol{N}(\boldsymbol{q}, \dot{\boldsymbol{q}}) + \boldsymbol{G}(\boldsymbol{q})$, the acceleration vector $\ddot{\boldsymbol{q}}$ can then be obtained from

$$\ddot{\boldsymbol{q}} = \boldsymbol{M}^{-1}(\boldsymbol{q})(\tau - \boldsymbol{h}(\boldsymbol{q}, \dot{\boldsymbol{q}})) \tag{77}$$

where the values of $\boldsymbol{q}$, $\dot{\boldsymbol{q}}$, and $\tau$ are assumed to be known at each time instant. Numerical integration is then used to find $\boldsymbol{q}$ and $\dot{\boldsymbol{q}}$ for the next time step. To do this, we need first to be able to compute $\boldsymbol{M}(\boldsymbol{q})$ and $\boldsymbol{h}(\boldsymbol{q}, \dot{\boldsymbol{q}})$. Numerical procedures[17] can enable us to compute these quantities numerically for given values of $\boldsymbol{q}$ and $\dot{\boldsymbol{q}}$. Based on the presented Newton-Euler formulation, a computer routine can be used to compute the Cartesian space force/torque vector $\tau$ for given Cartesian space position, velocity and acceleration vectors $\boldsymbol{q}$, $\dot{\boldsymbol{q}}$, $\ddot{\boldsymbol{q}}$. Setting $\ddot{\boldsymbol{q}}$ equal to zero when calling the routine will return the numerical value of the Coriolis, centrifugal, and gravity force/torque $\boldsymbol{h}(\boldsymbol{q}, \dot{\boldsymbol{q}})$. Similarly, calling the routine with $\ddot{\boldsymbol{q}}$ having zero elements except the $i$th element which is set to be unity, with $\dot{\boldsymbol{q}}$ and g being equal to zero, will return the numerical value of the $i$th column of the $\boldsymbol{M}(\boldsymbol{q})$ matrix. This procedure is repeated for $i=1, \ldots, 6$ to compute the six columns of the $\boldsymbol{M}(\boldsymbol{q})$ matrix.

## 9. INCLUSION OF ACTUATOR DYNAMICS

In a previous section, we showed that the rigid body dynamics of Stewart Platform mechanism of interest are modeled by second order nonlinear, coupled differential equations represented by Equation (76). We can transform this equation to joint space using Equations (23) and (74), yielding

$$\boldsymbol{M}_j(\boldsymbol{q})\ddot{\boldsymbol{l}}+\boldsymbol{N}_j(\boldsymbol{q}, \dot{\boldsymbol{q}})+\boldsymbol{G}_j(\boldsymbol{q})=\boldsymbol{F} \tag{78}$$

where $\boldsymbol{F}$ is the 6-vector of the input forces in joint space,

$$\boldsymbol{M}_j(\boldsymbol{q})=\boldsymbol{J}^T\boldsymbol{M}(\boldsymbol{q})\boldsymbol{J} \tag{79}$$

$$\boldsymbol{N}_j(\boldsymbol{q}, \dot{\boldsymbol{q}})=\boldsymbol{J}^T\boldsymbol{N}(\boldsymbol{q}, \dot{\boldsymbol{q}})-\boldsymbol{J}^T\boldsymbol{M}(\boldsymbol{q})\boldsymbol{J}\frac{d\boldsymbol{J}^{-1}}{dt}\dot{\boldsymbol{q}} \tag{80}$$

and

$$\boldsymbol{G}_j(\boldsymbol{q})=\boldsymbol{J}^T\boldsymbol{G}(\boldsymbol{q}) \tag{81}$$

Once the dynamic equations are expressed in joint space, the actuator dynamics can be added easily.

For the six motor-ballscrew-nut drives powering the struts, assuming identical links and viscous damping, the actuator mechanical dynamic equation can be written in matrix form as

$$\boldsymbol{M}_a\ddot{\boldsymbol{l}}+\boldsymbol{V}_a\dot{\boldsymbol{l}}+\boldsymbol{K}_a\boldsymbol{F}=\tau_m \tag{82}$$

where

$$\boldsymbol{M}_a=M_a\boldsymbol{I}_{6\times6}=\frac{2\pi}{np}(J_s+n^2J_m)\boldsymbol{I}_{6\times6} \tag{83}$$

$$\boldsymbol{V}_a=V_a\boldsymbol{I}_{6\times6}=\frac{2\pi}{np}(b_s+n^2b_m)\boldsymbol{I}_{6\times6} \tag{84}$$

$$\boldsymbol{K}_a=K_a\boldsymbol{I}_{6\times6}=\frac{p}{2\pi n}\boldsymbol{I}_{6\times6} \tag{85}$$

$\boldsymbol{M}_a$ and $M_a$ are the actuator inertia matrix and element, $\boldsymbol{V}_a$ and $V_a$ are the actuator viscous damping coefficient matrix and element, and $\boldsymbol{K}_a$ and $K_a$ are the actuator gain matrix and element. $J_s$ and $J_m$ are the mass moments of inertia of the ballscrew and motor, $b_s$ and $b_m$ are the viscous damping coefficient of the ballscrew and motor, $p$ is the pitch of the ballscrew, and $n$ is the gear ratio. $\tau_m$ is the vector of motor torques.

Equation (82) can be combined with Equation (78) to form

$$\overline{\boldsymbol{M}}_j(\boldsymbol{q})\ddot{\boldsymbol{l}}+\overline{\boldsymbol{N}}_j(\boldsymbol{q}, \dot{\boldsymbol{q}})+\overline{\boldsymbol{G}}_j(\boldsymbol{q})=\tau_m \tag{86}$$

where

$$\overline{\boldsymbol{M}}_j(\boldsymbol{q})=\boldsymbol{K}_a\boldsymbol{J}^T\boldsymbol{M}(\boldsymbol{q})\boldsymbol{J}+\boldsymbol{M}_a \tag{87}$$

$$\overline{\boldsymbol{N}}_j(\boldsymbol{q}, \dot{\boldsymbol{q}})=\boldsymbol{K}_a\boldsymbol{J}^T\boldsymbol{N}(\boldsymbol{q}, \dot{\boldsymbol{q}})+\left(\boldsymbol{V}_a-\boldsymbol{K}_a\boldsymbol{J}^T\boldsymbol{M}(\boldsymbol{q})\boldsymbol{J}\frac{d\boldsymbol{J}^{-1}}{dt}\boldsymbol{J}\right)\boldsymbol{J}^{-1}\dot{\boldsymbol{q}} \tag{88}$$

$$\overline{\boldsymbol{G}}_j(\boldsymbol{q})=\boldsymbol{K}_a\boldsymbol{J}^T\boldsymbol{G}(\boldsymbol{q}) \tag{89}$$

Equation (86) presents the combined rigid body and actuator dynamics transformed to joint space.

Equivalently, for the purpose of simulating the combined system, Equation (86) can also be expressed in Cartesian space as

$$\overline{\boldsymbol{M}}_c(\boldsymbol{q})\ddot{\boldsymbol{q}}+\overline{\boldsymbol{N}}_c(\boldsymbol{q}, \dot{\boldsymbol{q}})+\overline{\boldsymbol{G}}_c(\boldsymbol{q})=\tau_m \tag{90}$$

where

$$\overline{\boldsymbol{M}}_c(\boldsymbol{q})=\boldsymbol{K}_a\boldsymbol{J}^T\boldsymbol{M}(\boldsymbol{q})+\boldsymbol{M}_a\boldsymbol{J}^{-1} \tag{91}$$

$$\overline{\boldsymbol{N}}_c(\boldsymbol{q}, \dot{\boldsymbol{q}})=\boldsymbol{K}_a\boldsymbol{J}^T\boldsymbol{N}(\boldsymbol{q}, \dot{\boldsymbol{q}})+\left(\boldsymbol{V}_a\boldsymbol{J}^{-1}+\boldsymbol{M}_a\frac{d\boldsymbol{J}^{-1}}{dt}\right)\dot{\boldsymbol{q}} \tag{92}$$

$$\overline{\boldsymbol{G}}_c(\boldsymbol{q})=\boldsymbol{K}_a\boldsymbol{J}^T\boldsymbol{G}(\boldsymbol{q}) \tag{93}$$

The actuator electrical dynamics are also formulated in joint space and can be described by the following equations assuming brush type DC motor

$$\tau_m=\boldsymbol{K}_t\,\boldsymbol{i} \tag{94}$$

$$\boldsymbol{L}\frac{d\boldsymbol{i}}{dt}+\boldsymbol{R}\,\boldsymbol{i}+\boldsymbol{K}_b\dot{\theta}_m=\boldsymbol{v} \tag{95}$$

$\boldsymbol{K}_t$, $\boldsymbol{L}$, $\boldsymbol{R}$, and $\boldsymbol{K}_b$ are the motor torque matrix, motor armature inductance matrix, motor armature resistance matrix and motor back emf matrix respectively. $\boldsymbol{i}$ and $\boldsymbol{v}$ are the 6-vectors of motor currents and voltages, respectively. $\dot{\theta}_m$ is the motor angular velocity vector, and is related to joint space velocity vector by

$$\dot{\theta}_m=\frac{2\pi n}{p}\dot{\boldsymbol{l}} \tag{96}$$

Using Equations (90), (94), (95) and (96), the simulation block diagram of the system which includes the actuator dynamics will be as shown in Figure 7. In this figure, we assume a direct drive ($n=1$ in Equations (90)). The resulting dynamic system is described by a vector third order differential equation, with the motor voltage vector $\boldsymbol{v}$ as the

https://doi.org/10.1017/S0263574703005046 Published online by Cambridge University Press

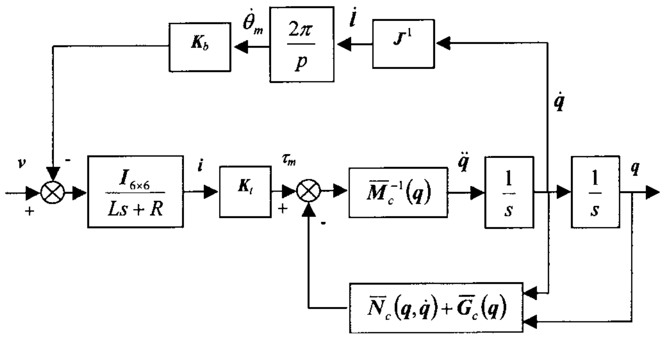


Fig. 7. Simulation block diagram of Stewart platform mechanism dynamics including actuator dynamics.

input to the system. We use Equation (90) which describes the system dynamics in Cartesian space, rather than Equation (86) which describes the system dynamics in joint space, to simulate the rigid-body dynamics to avoid using forward kinematics to obtain $\boldsymbol{q}$ from $\boldsymbol{l}$, $\boldsymbol{q}$ being needed for computing the rigid body dynamics.

### *9.1. Simulation study*

To see the significance of the different terms in the obtained dynamic equations, computer simulation is used to compute the inverse dynamics of the combined system including actuator dynamics. Inertial, velocity and gravity terms of the combined system as reflected on the machine prismatic joint axes are evaluated. A circular trajectory of 40 cm radius traversed in a plane tilted with respect to the X-Y plane, with a speed of 12 m/min, is used in the evaluation. A trapezoidal velocity profile with commanded constant acceleration and deceleration at the beginning and end of the trajectory is used to simulate machine motion. The orientation of the platform is kept unchanged and horizontal during this motion.

Figure 8 shows the results of this simulation for the six axes of the machine. Because the traversed trajectory is a circular one, the dynamic terms appear to vary sinusoidally. The gravity term has a significantly larger magnitude of variation due to the relatively large trajectory traversed and correspondingly large change in strut inclination. The damping term, which depends on the traversing speed, shows significant variation also. The actuator and rigid body inertial term variations are small compared to the previously mentioned terms, except at the beginning and end of the trajectory, where the acceleration components are higher. Coriolis and centrifugal term variations were insignificant during this trajectory.

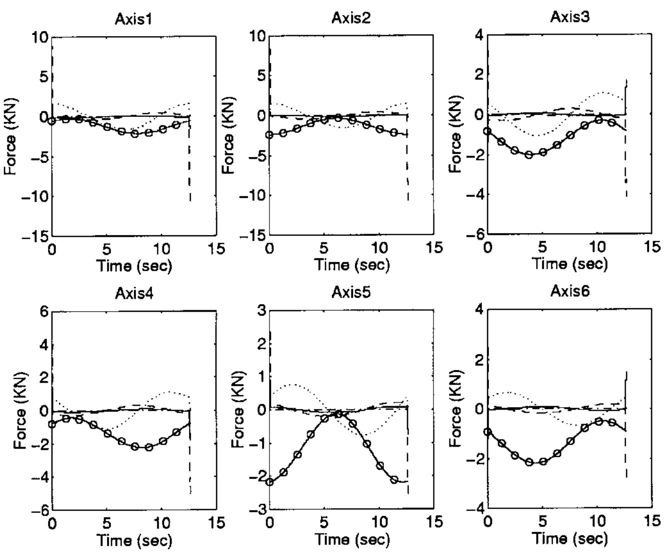


Fig. 8. Joint force components for tilted circular trajectory: Radius=40 cm, Speed=12 m/min, '__' rigid body inertial terms, '--' actuator inertial terms, '-.' Coriolis and centrifugal terms, '. .' actuator damping terms, '-o-' gravity terms.

## 10. INCLUSION OF JOINT FRICTION

Friction has a significant impact on the dynamics of mechanisms in general. In conventional machine tools, low velocity friction is important when a feed drive axis reverses direction, and is one of the main sources of motion control errors. The kinematics of machine tools with conventional architectures are relatively simple as compared to those of robotic mechanisms in general. This makes prediction of the instants of direction reversal in machine tool feed drives easier. For example, two dimensional circular contours on x-y tables result in direction reversals at the beginning of each quadrant of the circle. In contrast, for Stewart Platform mechanisms, both powered and unpowered joints will experience direction reversals even with simple straight-line trajectories. Friction analysis of the different joints therefore requires availability of accurately modeled relative motions at the joints.

Direction reversal is easy to predict for single degree-of-freedom (DOF) joints such as prismatic and revolute joints. A two DOF universal joint can also be viewed as two single DOF joints connecting three links as was presented earlier. On the other hand, relative motion of a three DOF unpowered spherical joint involves three-dimensional motion. For the purpose of analyzing friction, the spherical joint may be viewed as a revolute joint having a pure rotation about an instantaneous screw axis.[18] The instantaneous screw axis is represented by a unit vector $\boldsymbol{s}$, which can be computed from

$$\boldsymbol{s}=\frac{\boldsymbol{\omega}_r}{\|\boldsymbol{\omega}_r\|} \tag{97}$$

where $\boldsymbol{\omega}_r$ is the relative angular velocity vector between the ball and the socket.

In the following development, a Coulomb friction model for the unpowered joints is added to the dynamic equations of the Stewart Platform mechanism previously derived, assuming that spherical platform and base joints are used for each strut. We assume that the friction at the joints depends on the relative velocities as well as on the reaction forces at these joints. Accurate relative velocity models at the joints were presented in the kinematic analysis section. Analysis of the transmitted forces between the struts and the moving platform is also presented previously.

With this knowledge of the relative velocity, and assuming for now that the reaction forces at the joints are known, we proceed to compute the friction torque vectors $\tau_{ai}$ and $\tau_{bi}$ that act on the $i$th strut at joints $a_i$ and $b_i$

https://doi.org/10.1017/S0263574703005046 Published online by Cambridge University Press

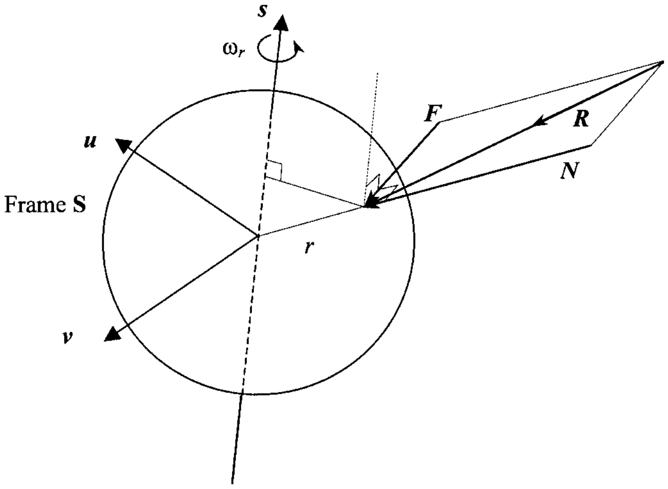


Fig. 9. Force components acting on the ball of a spherical joint.

respectively. Figure 9 shows the reaction force components transmitted from the base/platform to the ball of the respective spherical joint. We assume here that the ball is rigidly attached to the strut while the socket is rigidly attached to the base/platform. For a frictionless joint, the reaction force $\boldsymbol{R}$ transmitted through the joint will be oriented radially to the ball. However, as shown in Figure 9, in the presence of a friction force component $\boldsymbol{F}$, which is tangent to the ball at the point of contact and normal to the instantaneous screw axis $\boldsymbol{s}$, $\boldsymbol{R}$ will not be radial. Instead, $\boldsymbol{R}$ can be resolved into the friction force component $\boldsymbol{F}$ and another normal force component $\boldsymbol{N}$ that passes through the center of the joint.

$$\boldsymbol{R}=\boldsymbol{F}+\boldsymbol{N} \tag{98}$$

Assuming Coulombic friction, the magnitudes of $\boldsymbol{F}$ and $\boldsymbol{N}$ are related by

$$F=\mu N \tag{99}$$

where $\mu$ is the coefficient of friction at the joint. Also, since the magnitudes of $\boldsymbol{R}$, $\boldsymbol{F}$ and $\boldsymbol{N}$ are related by $R^2=F^2+N^2$, the magnitudes of $\boldsymbol{F}$ and $\boldsymbol{N}$, in terms of the magnitude of $\boldsymbol{R}$ and the coefficient of friction $\mu$, are obtained as

$$F=\frac{\mu}{\sqrt{1+\mu^2}}R \tag{100}$$

$$N=\frac{1}{\sqrt{1+\mu^2}}R \tag{101}$$

The force system acting on the ball of the spherical joint can be replaced by an equivalent reaction force $\boldsymbol{R}$ at the center of the ball and a friction torque $\tau_f$. It can be shown that $\tau_f$ could be obtained from

$$\boldsymbol{\tau}_f=-\frac{r}{N}\boldsymbol{R}\times\boldsymbol{F} \tag{102}$$

where $r$ is the radius of the ball. To find this friction torque $\tau_f$, we need to determine the direction of the friction force vector $\boldsymbol{F}$. For this purpose we will define a coordinate frame **S** that is aligned with the screw axis $\boldsymbol{s}$ as shown in Figure 9. Axis $\boldsymbol{s}$ will form one axis of this frame. Axis $\boldsymbol{u}$ is defined to be normal to the plane formed by $\boldsymbol{s}$ and $\boldsymbol{k}$, where $\boldsymbol{k}$ is a unit vector along the Z-axis of the world coordinate system **W**. Therefore, the transformation matrix from frame **S** to the world frame **W** is constructed as

$$^{W}\boldsymbol{T}_S=(\boldsymbol{u}\ \ \boldsymbol{v}\ \ \boldsymbol{s})=\left(\frac{\boldsymbol{k}\times\boldsymbol{s}}{\|\boldsymbol{k}\times\boldsymbol{s}\|}\quad \boldsymbol{s}\times\left(\frac{\boldsymbol{k}\times\boldsymbol{s}}{\|\boldsymbol{k}\times\boldsymbol{s}\|}\right)\quad \boldsymbol{s}\right) \tag{103}$$

Since the friction force $\boldsymbol{F}$ is normal to axis $\boldsymbol{s}$, it will be in the $u$-$v$ plane and can be stated in frame **S** as

$$^{s}\boldsymbol{F}=F(\cos\theta_f,\ \sin\theta_f,\ 0)^T \tag{104}$$

where $\theta_f$ is the angle that $\boldsymbol{F}$ makes with the $u$-axis. Using the transformation (103), the components of $\boldsymbol{R}$ along axes $\boldsymbol{u}$, $\boldsymbol{v}$ and $\boldsymbol{s}$ are determined as $R_u$, $R_v$ and $R_s$ respectively. Since $\boldsymbol{F}$ is normal to axis $\boldsymbol{s}$, only $R_u$ and $R_v$ will be contributing to $\boldsymbol{F}$. Hence the magnitude of $\boldsymbol{F}$ can be written as

$$F=|R_u\cos\theta_f+R_v\sin\theta_f| \tag{105}$$

Since the magnitude of $\boldsymbol{F}$ is known from Equation (100), Equation (105) can be solved for $\theta_f$, yielding

$$\theta_f=2\tan^{-1}\frac{R_v\pm\sqrt{R_u^2+R_v^2-F^2}}{R_u+F} \tag{106}$$

This equation indicates that there are two possible solutions. The solution that results in a friction torque component opposing $\boldsymbol{\omega}_r$ is the correct one. Once $^{S}\boldsymbol{F}$ is determined, it can be transformed back to frame **W** using the transformation Equation (103), and then used to compute the friction torque $\tau_f$ using Equation (102).

Once joint friction torques are computed, $\tau_{ai}$ and $\tau_{bi}$ at the platform and base respectively, they should be added to the left hand side of the moment equation in Equation (55), and hence subtracted from the definition of $\boldsymbol{N}_i$ in Equation (57). Also, friction torque vectors equal and opposite to $\tau_{ai}$ will be acting on the platform at $a_i$ for $i=1\ldots6$. Therefore, $\sum_{i=1}^{6}\tau_{ai}$ should be subtracted from the left hand side of Equation (64), and hence subtracted from the lower element of vector $\boldsymbol{C}$ in Equation (69). After adding these terms, the dynamic equation can be rewritten as

$$\tau=\boldsymbol{M}(\boldsymbol{q})\ddot{\boldsymbol{q}}+\boldsymbol{N}(\boldsymbol{q},\dot{\boldsymbol{q}})+\boldsymbol{G}(\boldsymbol{q})+\boldsymbol{T}_f(\boldsymbol{q},\dot{\boldsymbol{q}},\ddot{\boldsymbol{q}}) \tag{107}$$

where $\boldsymbol{T}_f(\boldsymbol{q},\dot{\boldsymbol{q}},\ddot{\boldsymbol{q}})$ is a 6-vector of joint friction torques and is given by

$$\boldsymbol{T}_f(\boldsymbol{q},\dot{\boldsymbol{q}},\ddot{\boldsymbol{q}})=-\boldsymbol{J}_2^{-T}\boldsymbol{C}_f \tag{108}$$

where $\boldsymbol{C}_f$ is given by

$$\boldsymbol{C}_f=\begin{pmatrix} -\sum_{i=1}^{6}\boldsymbol{N}_{fi}\times\boldsymbol{n}_i/l_i \\ \sum_{i=1}^{6}(\boldsymbol{N}_{fi}\times\boldsymbol{n}_i/l_i)\times{}^{w}\boldsymbol{R}_p\,{}^{p}\boldsymbol{a}_i-\sum_{i=1}^{6}\tau_{ai}\end{pmatrix} \tag{109}$$

and

$$\boldsymbol{N}_{fi}=-\tau_{bi}-\tau_{ai} \tag{110}$$

https://doi.org/10.1017/S0263574703005046 Published online by Cambridge University Press

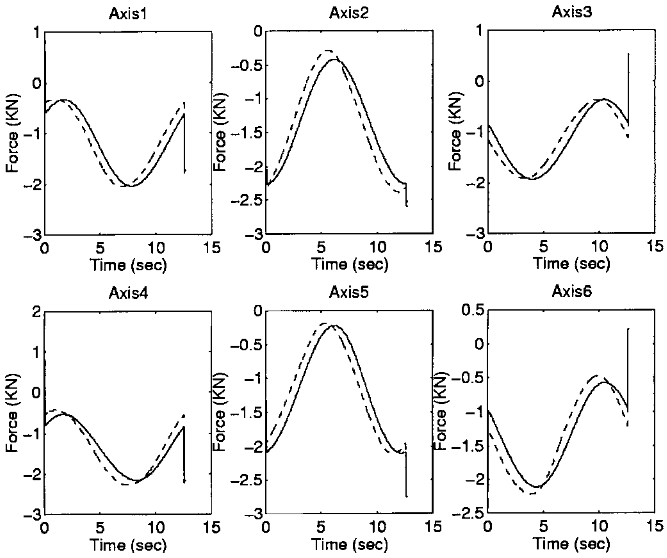


Fig. 10. Joint force components for tilted circular trajectory: Radius=40 cm, Speed=12 m/min, '__' frictionless joints, '--' spherical joints with friction.

The dependence of the friction torques $\tau_{ai}$ and $\tau_{bi}$ on the reaction forces at the joints will render the dynamic equations implicit. Iterative procedures should be employed in this case to solve the resulting equations. The reaction force $\boldsymbol{R}_{ai}$ at joint $a_i$ is simply obtained by adding $\boldsymbol{F}_i^n$ to $\boldsymbol{F}_i^a$, given by Equations (61) and (62), respectively. On the other hand, the reaction force $\boldsymbol{R}_{bi}$ at joint $b_i$ can be obtained by performing a force balance on strut $i$, which gives $\boldsymbol{R}_{bi}$ as

$$\boldsymbol{R}_{bi}=m_1\,\boldsymbol{a}_{i1}+m_2\,\boldsymbol{a}_{i2}-\boldsymbol{F}_i^n-\boldsymbol{F}_i^a-m_1\,\boldsymbol{G}-m_2\,\boldsymbol{G} \quad (111)$$

### *10.1. Simulation study of friction effects*

In this study the rigid body dynamics as represented by Equation (78) are simulated with and without spherical joint friction effects. The circular trajectory considered previously is used again in this study. A friction coefficient of 0.1 is assumed in this simulation. Figure 10 shows the actuator force requirements for the two cases of frictionless spherical joints and spherical joints with friction. Since actuator dynamic effects are not included in Equation (78), the actuator forces here are mainly due to the gravity effect. The presence of joint friction results in a maximum difference of about 0.3 KN for some of the actuators. In one half of the tilted trajectory, the platform is moving upward and hence extra forces are needed in the presence of friction. In the other half, the platform is moving downward and hence a smaller force is needed since friction is helping the actuators in overcoming gravity. The result shown here indicates that friction effects are significant.

## 12. CONCLUSIONS

In this paper, a study of the kinematics of a Stewart Platform mechanism has been presented. Closed form solutions for the inverse position, rate and acceleration kinematics are presented. As part of these solutions, the inverse Jacobian matrix of the mechanism, and its time derivative, are derived. Since there is no closed form solution for the forward kinematic problem for the general class of Stewart Platforms, we investigate also the use of a numerical iterative solution for this problem based on the Newton-Raphson method. It is shown, through a numerical example, that an acceptable solution could be reached after a few iterations, providing that an initial guess close enough to the actual solution is available. Finally, kinematic analyses for the angular velocities and accelerations of the links and unpowered joints are presented. It is shown that the angular velocities and accelerations of the links are different for different types of unpowered joints.

A study of the dynamics of Stewart Platform mechanisms is also presented. A dynamic model based on the Newton-Euler formulation for a general class of Stewart Platform mechanisms is derived. The Newton-Euler formulation results in an efficient procedure to compute the inverse dynamics of the mechanism. The dynamic equations derived thus in Cartesian space are transformed to joint space in order to add actuator dynamic effects including actuator electricat as well as mechanical dynamics. Also, effects of unpowered joint friction are added to the derived rigid body dynamic model. Friction effect are seen to be significant for realistic friction levels, suggesting that friction compensation should be an explicit objective of control.

## Acknowledgements

The authors gratefully acknowledge the support of the National Science Foundation (NSF) under Grant No. DMI – 9632986 and the National Institute of Standards and Technology (NIST) under Grant No. 70NANB6H0080. The first author also acknowledges the financial support from the United Arab Emirates University. The authors also wish to thank Mr. Denis Garagic from the Ohio State University for his valuable comments and review of the paper.

## References

1. V.E. Gough and S.G. Whitehall, "Universal Tyre Test Machine", *Proc. 9th International Technical Congress F.I.S.I.T.A.* (1962) pp. 117–137.
2. D. Stewart, "A Platform with Six Degrees of Freedom", *Proceedings of the Institution of Mechanical Engineers*, London **180**, No. 15, 371–386 (1965).
3. K.H. Hunt, *Kinematic Geometry of Mechanisms* (Oxford University, London, 1978).
4. Z. Geng and L.S. Haynes, "Six-Degree-of-Freedom Active Vibration Isolation Using a Stewart Platform Mechanism", *J. Robotic Systems* **10**, No. 5, 725–744 (1993).
5. P. Nanua, K.J. Waldron and V. Murthy, "Direct Kinematic Solution of a Stewart Platform", *IEEE Trans. on Robotics and Automation* **6**, No. 4, 438–443 (1990).
6. W.Q.D. Do and D.C.H. Yang, "Inverse Dynamic Analysis and Simulation of a Platform Type of Robot", *J. Robotic Systems* **5**, No. 3, 209–227 (1988).
7. Z. Ji, "Study of the Effect of Leg Inertia in Stewart Platform", *Proc. of the IEEE Conf. on Robotics and Automation* (1993) **Vol. 1**, pp. 212–226.
8. B. Dasgupta and T.S. Mruthyunjaya, "A Newton-Euler Formulation for the Inverse Dynamics of the Stewart Platform Manipulator", *Mechanism and Machine Theory* **33**, No. 8, 1135–1152 (1998).
9. C.C. Nguyen and F.J. Pooran, "Dynamic Analysis of a 6 DOF CKCM Robot End-Effector for Dual-Arm Telerobot Systems", *Robotics and Autonomous Systems* **5**, 377–394 (1989).

10. Z. Geng, L.S. Haynes, J.D. Lee and R.L. Carroll, "On the Dynamic Model and Kinematic Analysis of a Class of Stewart Platforms", *Robotics and Autonomous Systems* **9**, 237–254 (1992).
11. G. Lebret, K. Liu and F.L. Lewis, "Dynamic Analysis and Control of a Stewart Platform Manipulator", *J. Robotic Systems* **10**, No. 5, 629–655 (1993).
12. O. Ma and J. Angeles, "Archticture Singudarities of Parallel Manipulators", *Int. J. of Robotics and Automation* **7**, No. 1, 23–29 (1992).
13. M.L. Husty, An Algorithm for Solvmg the Direct Kinematics of General Stewart-Gough Platform, *Mech. Mach. Theory* **31**, No. 4, 365–380, (1996).
14. C.W. Wampler, Forward Displacement Analysis of General Six-in-Parallel SPS (Stewart) Platform Manipulators Using Soma Coordinates, *Mech. Mach. Theory* **31**, No. 3, 331–337 (1996).
15. C.E. Wilson and J.P. Sadler, *Kinematics and Dynamics of Machinery* (Harper Collins College Publishers, New York, NY, 1993).
16. K. Harib, "Dynamic Modeling and Control of Stewart Platform-Based Machine Tools", *Ph.D. Thesis* (Department of Mechanical Engineering, The Ohio State University, Columbus, Ohio, 1997).
17. M.W. Walker and D.E. Orin, "Efficient Dynamic Computer Simulation of Robotic Mechanisms", *J. of Dynamic System, Measurement, and Control* **104**, 205–211 (1982).
18. L.J. Gutkowski, "A General, Robust Procedure for the Kinematic and Friction Force Analysis of Single Loop, One DOF Spatial Mechanism", *Ph.D. Thesis* (Department of Mechanical Engineering, TheOhio State University, Columbus, Ohio, 1990).

## APPENDIX

The constant mass moment of inertia tensor ${}^{xyz}\bar{\boldsymbol{I}}$ of a rigid body, stated with reference to a body coordinate frame *x-y-z* at the center of mass, can be transformed to a non rotating coordinate frame *X-Y-Z* as

$$\bar{\boldsymbol{I}}={}^{XYZ}\boldsymbol{R}_{xyz}\,{}^{xyz}\bar{\boldsymbol{I}}\,{}^{XYZ}\boldsymbol{R}_{xyz}^{T} \tag{a}$$

where ${}^{XYZ}\boldsymbol{R}_{xyz}$ is a rotation matrix describing the orientation of frame *x-y-z* with reference to frame *X-Y-Z*. One way to obtain relation (a) is by using the fact that the kinetic energy of a rotating rigid body is the same in all coordinate systems.

$$K=\frac{1}{2}\,{}^{xyz}\omega^{T}\,{}^{xyz}\bar{\boldsymbol{I}}\,{}^{xyz}\omega=\frac{1}{2}\,\omega^{T}\,\bar{\boldsymbol{I}}\,\omega \tag{b}$$

is the angular velocity vector of the body stated in frame *x-y-z*, which can be transformed to frame *X-Y-Z* as $\omega={}^{XYZ}\boldsymbol{R}_{xyz}\,{}^{xyz}\omega$. By recalling the orthogonal property of ${}^{XYZ}\boldsymbol{R}_{xyz}$ which states ${}^{XYZ}\boldsymbol{R}_{xyz}^{-1}={}^{XYZ}\boldsymbol{R}_{xyz}^{T}$, one can verify relation (a) quite easily.

Now, let *x*, *y*, and *z* be the principal axes of the rigid body, with $\bar{I}_{xx}$, $\bar{I}_{yy}$, and $\bar{I}_{zz}$ being the mass moment of inertia components about the principal axes, respectively, and let ${}^{XYZ}\boldsymbol{R}_{xyz}$ be defined as ${}^{XYZ}\boldsymbol{R}_{xyz}=[\boldsymbol{n}\ \ \boldsymbol{u}\ \ \boldsymbol{v}]$, where $\boldsymbol{n}$, $\boldsymbol{u}$, and $\boldsymbol{v}$ are unit vectors along the *x*, *y*, and *z* axes, respectively, and stated with reference to frame *X-Y-Z*. Equation (a) will expand to

$$\bar{\boldsymbol{I}}=\bar{I}_{xx}\,\boldsymbol{n}\,\boldsymbol{n}^{T}+\bar{I}_{yy}\,\boldsymbol{u}\,\boldsymbol{u}^{T}+\bar{I}_{zz}\,\boldsymbol{v}\,\boldsymbol{v}^{T} \tag{c}$$

Further, assuming an axisymmetric body, with $\bar{I}_{xx}=\bar{I}_{aa}$ and $\bar{I}_{yy}=\bar{I}_{zz}=\bar{I}_{nn}$, we get

$$\bar{\boldsymbol{I}}=\bar{I}_{aa}\,\boldsymbol{n}\,\boldsymbol{n}^{T}+\bar{I}_{nn}(\boldsymbol{I}_{3\times 3}-\boldsymbol{n}\,\boldsymbol{n}^{T}) \tag{d}$$

where $\boldsymbol{I}_{3\times3}$ is the $3\times3$ identity matrix. Once again we use the orthogonal property of ${}^{XYZ}\boldsymbol{R}_{xyz}$ which states $\boldsymbol{n}\,\boldsymbol{n}^{T}+\boldsymbol{u}\,\boldsymbol{u}^{T}+\boldsymbol{v}\,\boldsymbol{v}^{T}=\boldsymbol{I}_{3\times3}$.

By noting that $\boldsymbol{n}\,\boldsymbol{n}^{T}\alpha=(\boldsymbol{n}\cdot\alpha)\boldsymbol{n}$, and $(\boldsymbol{I}_{3\times3}-\boldsymbol{n}\,\boldsymbol{n}^{T})\alpha=\boldsymbol{n}\times(\alpha\times\boldsymbol{n})$ which can be verified by expanding and comparing terms, $\bar{\boldsymbol{I}}\,\alpha$, for an axisymmetric body, can be written as

$$\bar{\boldsymbol{I}}\,\alpha=\bar{I}_{aa}(\boldsymbol{n}\cdot\alpha)\boldsymbol{n}+\bar{I}_{nn}\,\boldsymbol{n}\times(\alpha\cdot\boldsymbol{n}) \tag{e}$$

Similarly, $\bar{\boldsymbol{I}}\,\omega\times\omega$ will reduce to

$$\bar{\boldsymbol{I}}\,\omega\times\omega=(\bar{I}_{aa}-\bar{I}_{nn})(\boldsymbol{n}\cdot\omega)\boldsymbol{n}\times\omega \tag{f}$$

https://doi.org/10.1017/S0263574703005046 Published online by Cambridge University Press